RESEARCH ARTICLE

Journal of Cellular Biochemistry WILEY

Effects of dexmedetomidine on glioma cells in the presence or absence of cisplatin

Hui Yang[1] | Yudan Chen[2] | Hui Yan[3] | Hao Wu[3] 🆔

[1]Department of Anesthesiology, The 3rd Xiangya Hospital of Central South University, Chang Sha, China

[2]Department of Hemodialysis, The 3rd Xiangya Hospital of Central South University, Chang Sha, China

[3]Department of Neurosurgery, The 3rd Xiangya Hospital of Central South University, Chang Sha, China

Correspondence
Hao Wu, Department of Neurosurgery, The 3rd Xiangya Hospital of Central South University, Tong Zi Po Road, No. 138, Yue Lu, 410006 Chang Sha, China.
Email: 57299239@qq.com

Abstract

With the extensive use of dexmedetomidine (Dex) in the surgical resection of tumours for its potent sedative and analgesic properties, its effects on various properties of tumours have received increased attention. The study described herein aimed to investigate the effects of Dex on glioma cells in the presence or absence of cisplatin (DDP). Glioma U251 and U87MG cells were treated with different doses (1-50 nM) of Dex for 12 hours, then recultured in a Dex-free medium. In addition, Dex was added to U251 and U87MG cells 12 hours before or simultaneously with a 12-hour DDP treatment. Treatment with Dex increased the viability of both cell lines; this effect continued for at least 24 hours after Dex was removed. A cell invasion assay indicated that Dex inhibited cell invasion at 50 nM, but not at 10 nM. Western blot analysis showed that Dex increased the expression of phosphorylated extracellular-signal-regulated kinase 1/2, phosphoitide 3-kinase and p-AKT, but decreased ROCK protein levels at a dose of 50 nM. Intracellular Ca^{2+} concentration was decreased by Dex in a dose-dependent manner. DDP toxicity was attenuated by 10 nM Dex added either before or with DDP treatment. However, pretreatment with 50 nM Dex instead enhanced the toxicity of DDP. Single-dose treatment with Dex did not significantly change glioma volume in nude mice, but changed the expression of Ki67 and matrix metalloproteinase-3 in the tumour. In conclusion, this study provides evidence of the regulatory effects of Dex on proliferation, invasion and chemosensitivity of glioma cells, and outlines potential mechanisms for these effects.

KEYWORDS
cell invasion, cell migration, cisplatin α2-AR, dexmedetomidine, glioma

1 | INTRODUCTION

Glioma is the most medically challenging malignant brain tumour, with highly proliferative, invasive and drug-resistant hallmarks. The incidence of glioma is also relatively high, presenting in 5.26 per 100 000 individuals.[1] The current standard of treatment requires surgical resection followed by radiotherapy and chemotherapy, but the rate of survival remains poor. The median overall survival rates for low-grade gliomas (WHO grade II), anaplastic gliomas (WHO grade III) and glioblastomas (GBM, WHO IV) are 78.1, 37.6 and 14.4 months, respectively.[2] The refractory character of glioma is indeed the major cause of treatment failure, but many other factors also influence therapeutic outcome. An increasing number of studies indicate that many anaesthetics and analgesics used during or after the surgical excision exert significant effects on various

hallmarks of tumours.[3-5] Tramadol, a non-opioid central analgesic, attenuates the sensitivity of glioblastoma to the chemotherapy drug temozolomide through the suppression of Cx43-mediated gap junction intercellular communication.[3] In contrast, research has suggested that these types of drugs, such as propofol, lidocaine, sevoflurane and thiopental, may suppress the proliferation and invasion of glioma cells and, therefore, be beneficial in the control of cancer progression.[5-8] These varying effects may be due to different specific biological effects. Thus, specific study is necessary to determine the effects of each individual drug.

Dexmedetomidine (Dex), a selective agonist of the α_2-adrenoceptor (α_2-AR), has been increasingly used during surgical operations for its sedative, analgesic, anxiolytic and sympatholytic effects. Dex is popular not only for its synergistic anaesthetic effect with other anaesthetics, but also for the strong protection against tissue injury and function impairment it provides.[9,10] Protection by Dex appears to be primarily dependant on α_2-adrenergic activation, as blocking the α_2-AR abolishes these protective effects.[11] α_2-AR is a G_i-type G protein-coupled receptor that reduces intracellular cyclic AMP (cAMP) levels. Dex has high binding affinity for α_2-ARs (Dex > clonidine > tizanidine), activating them and subsequently modulating a host of signalling molecules. The well-identified basis for Dex-induced protection is the inhibition of nuclear factor-κB (NF-κB) by α_2-ARs, which reduces inflammatory response and oxidative stress.[12] However, this protection may be unfavourable for the elimination of a tumour by surgery. Lavon et al[13] found that Dex attenuates stress during surgery and further promotes metastasis of breast, lung and colon cancers in rodent models. An in vitro study also showed that Dex could promote the proliferation, migration and invasion of breast cancer cells through the activation of α_2-AR/ERK signalling.[14] In addition, the protective property of Dex diminishes cisplatin (DDP)-induced toxicity in the kidney through regulation of apoptosis and inflammation.[15] Hence, it is plausible that Dex could also protect cancer cells from DDP treatment. The present study aimed to investigate the effects of Dex on glioma cells in the presence or absence of DDP.

2 | MATERIALS AND METHODS

2.1 | Ethics statement

All animal experiments were approved by the Ethics Committee of Xiangya School of Medicine (Changsha, China), and were carried out in strict accordance with the recommendations laid out in the Guide for the Care and Use of Laboratory Animals of the National Institutes of Health.

2.2 | Cell culture and treatment

Human glioma cell lines, U251 and U87MG, were obtained from the American Type Culture Collection (ATCC) and maintained in a 37°C humidified atmosphere containing 5% CO_2 in Dulbecco's modified Eagle's media (DMEM; HyClone; Logan, UT) supplemented with 10% foetal bovine serum (FBS; HyClone; GE Healthcare Life Sciences), 2 mM L-glutamine (Sigma-Aldrich, Shanghai, China), 100 U/mL penicillin and 100 μg/mL streptomycin (Beyotime, Shanghai, China). For subsequent drug treatments and related tests, the cell medium was switched to DMEM (phenol red-free) supplemented with 3% FBS, 100 U/mL penicillin and 100 μg/mL streptomycin.

U251 and U87MG cells were treated with different doses of Dex (SML0956; Sigma-Aldrich) for 12 hours. Cells were then recultured in the Dex-free culture medium for 48 hours. Cell viability was assessed at different time points throughout. In addition, Dex was added to U251 and U87MG cells 12 hours before (processing mode one, P1) or simultaneously with (processing mode two, P2) treatment with 30 μM DDP (#P4394; Sigma-Aldrich) for 12 hours to determine the protective effect of Dex. A series of assays were performed immediately after P1 and 12 hours after P2. An ERK1/2 inhibitor MK-8353 (Selleck, Shanghai, China) and AKT inhibitor Perifosine (Selleck) were used at the dosage of 10 nM and 5 μM, respectively, in the study.

2.3 | Cell viability measurement

Cell viability was measured using cell counting kit-8 (CCK-8) (Sigma-Aldrich). In brief, 0.5×10^4 cells were seeded in each 96-well plate for 24 hours. After abovementioned treatment, CCK-8 reagents were added to each well at a final concentration of 10%. After incubating for 1 hour, optical density at 490 nm in each well was determined by an enzyme immunoassay analyser (Boehringer Mannheim ES700, UK).

2.4 | 5-Ethynyl-2′-deoxyuridine staining assay

Cells were treated with 5-ethynyl-2′-deoxyuridine (EdU) for 2 hours, washed with 3% BSA three times, and fixed with 4% paraformaldehyde for 10 minutes. After washing with 3% BSA three times, cells were permeabilised with 0.4% Triton X-100 for 15 minutes. Cells were then

incubated with EdU staining cocktail kept from lights at room temperature for 30 minutes. After washing with 3% BSA, samples were then counterstained with $1 \times$ Hoechst 33342 for 10 minutes. Images were acquired by fluorescence microscope.

2.5 | Flow cytometry method

Following cell treatment, cells were stained using Annexin V-FITC/PI Apoptosis Detection Kit I (Kaiji Biological Inc, Nanjing, China) according to the manufacturer's instructions. The rate of apoptosis was analysed using a dual laser flow cytometer (Becton Dickinson, San Jose, CA) and estimated using the ModFit LT software v. 1.0 (Verity Software House; Topsham, ME).

2.6 | Cell wound scratch assay

Glioma cells in logarithmic growth phase were plated in six-well plates. After >80% confluence of cells, a horizontal line was drawn at the bottom of each plate using 200-µL pipette tips. The plates were then rinsed three times with PBS to remove cells that had peeled off. After above-mentioned treatment, the distance of cell migration was determined by Image-Pro Plus 6.0 software (Media Cybernetics Inc, Rockville, MD) and cell migration rate was calculated by the following formula: cell migration rate (%) = [(initial distance − final distance)/initial distance] × 100%.

2.7 | Cell invasion assay

Cell invasion was evaluated using a Transwell chamber (Greiner; Monroe, NC) with 8-µm-pore filters. Glioma cells were placed in the upper chamber (100 µL/well) and then incubated at 37°C in 5% humidified CO_2 for 24 hours. The lower face of the filter was washed with PBS, and cells remaining on the upper side were removed using a cotton wool swab. Cells were then fixed with 2% paraformaldehyde for 10 minutes and stained with 0.1% crystal violet. The invaded cells in the lower chamber were counted in five random microscopic fields (×200).

2.8 | Western blot analysis

The glioma cells were lysed by radioimmunoprecipitation assay buffer containing protease inhibitors, and the cell lysates were separated by sodium dodecyl sulphate polyacrylamide gel electrophoresis on 10% polyacrylamide Tris-glycine gels. The proteins were electrophoretically transferred to a polyvinylidene difluoride membrane (Millipore). The membrane was blocked with 5% nonfat dry milk in 0.2% Tween-20 in Tris-buffered saline (TBS-T) and then incubated with antibodies as follows: anti-p-ERK1/2 antibody (ab201015; Abcam), anti-p-AKT antibody (ab66138; Abcam), anti-phospho-myosin light chain (p-MLC; ab2480; Abcam) and p-p65 (ab86299; Abcam) and glyceraldehyde 3-phosphate dehydrogenase (GAPDH) (ab8245; Abcam). After extensive washing (three times for 10 minutes each in TBS-T), horseradish peroxidase-conjugated secondary antibodies were added and incubated for 1 hour at 22°C. Blots were again washed three times for 10 minutes each in TBS-T, and immunoreactive bands were developed by enhanced chemiluminescence. GAPDH was used as a loading control.

2.9 | Measurement of intracellular Ca^{2+} concentration

Changes in intracellular free Ca^{2+} concentration ($[Ca^{2+}]_i$) were measured using fura-2 fluorescence dye (Sigma-Aldrich) at excitation wavelengths of 340 and 380 nm and an emission wavelength of 510 nm. Cells were cultured on cover slips in 35 mm² dishes and loaded with 5 µM fura-2 AM for 30 minutes. The dye was excited by alternatively using 340 nm (20 ms) and 380 nm wavelength (10 ms) light with a Xenon 75 W arc lamp. The emission fluorescence at 510 nm was detected using a photomultiplier tube. The 340-to-380-nm ratio (340/380) was calculated and used to represent the changes in $[Ca^{2+}]_i$. The fura-2 340/380 ratio is sensitive to changes in $[Ca^{2+}]_i$ at the nanomolar level. The signal-to-noise ratio was improved by averaging five consecutive 340/380 ratio readings. Emitted fluorescence was monitored using a high-performance CCD camera (Photometrics; AZ) attached to an inverted microscope (Olympus; Tokyo, Japan) and analysed with the MetaFluor system (Molecular Devices; PA). Fluorescence images were obtained at 1 second intervals, and background fluorescence was subtracted from raw signals at each excitation wavelength.

2.10 | Reactive oxygen species measurement

Intracellular reactive oxygen species (ROS) level was evaluated using 2,7′-dichlorodihydrofluorescein diacetate (H_2DCFDA; Invitrogen, Thermo Fisher Scientific; Waltham, MA). Following treatment, 3.5×10^5 cells were stained with 10 µM H_2DCFDA at 37°C for 10 minutes, and then washed twice with PBS. A fluorospectrophotometer (F-4000; Hitachi, Ltd, Tokyo, Japan) was used to

detect the fluorescence intensity of H_2DCFDA at an excitation wavelength of 488 nm and an emission wavelength of 525 nm.

2.11 | Tumour xenograft assay

For in vivo assays, nude male mice (4-6-week old) were purchased from an animal breeding facility (Slac Laboratory Animal Co, Changsha, China). Animals were maintained in a specific pathogen-free room in accordance with the institutional policies. Each mouse received a subcutaneous injection of U251 or U87MG cells (1×10^6). The mice were fed with pelleted standard feed and water and housed in steel cages at room temperature (23-26°C) under a 12/12 hours light/dark cycle. The nude mice 5 days after the implantation of U251 or U87MG cells received normal saline (as control), Dex (0.5 mg/kg, 0.1 mL/10 g; subcutaneous injection), DDP (4 mg/kg, 0.1 mL/10 g, intraperitoneal injection) or Dex + DDP per 5 days. Tumour volume (V) was calculated after the feeding for 1 month using the formula:

$$V = \frac{L \times W^2}{2},$$

where V is the tumour volume, L is the tumour length and W is the tumour width.

2.12 | Immunohistochemistry

Tissue sections were deparaffinised with xylene and rehydrated with ethanol, then treated with normal goat serum (10%) for 30 minutes to block nonspecific binding sites. Subsequently, the cells were incubated with primary antibodies targeting ki67 (ab15580; Abcam), active caspase-3 (ab2302; Abcam) and matrix metallo-proteinase-3 (MMP-3, ab53015; Abcam) at 4°C overnight. The primary antibodies were visualised by adding a secondary biotin-conjugated antibody, followed by an avidin/biotin/peroxidase complex (Vectastain ABC Elite kit; Vector Laboratories Inc, Burlingame, CA) and substrate (Vector NovaRED, Vectastain).

2.13 | Statistical analysis

Each experiment was repeated three times. Data are presented as means ± SD, and one-way analysis of variance were used to compare the means of independent samples. Statistical analyses were performed with SPSS 16.0 (SPSS Inc, Chicago, IL). $P < .05$ were considered statistically significant.

3 | RESULTS

3.1 | Effect of Dex on the growth of glioma cells and its underlying mechanisms

U251 and U87MG cells were treated with various doses of Dex (1, 10 and 50 nM) for 6 and 12 hours. Results showed that Dex increased the viabilities of both U251 and U87MG cells in a time-dependent manner, with the most significant effect at 10 nM ($P < 0.01$ or $P < 0.001$, Figure 1A). After incubation with Dex for 12 hours, to ensure each group has the same number of cells, Dex-treated cells were digested using pancreatic enzymes and then plated in a new 96-well plate without Dex. Glioma cells pretreated with Dex had higher cell viability than control cells that were never treated with Dex over 36 hours. The most significant difference between the Dex-treated groups and the control group was observed at 24 hours. Pretreatment with 50 nM Dex caused greater improvement on cell viability than the lower doses. Moreover, as indicated by Edu assay, the treatment with 10 nM Dex for 12 hours increased the proliferation of both U251 and U87MG cells (Figure 1B). In spite of24 and 36 hours after removing Dex, U251 and U87MG cells showed increased proliferation compared with control cells. Dex did not significantly affect the apoptosis rates of U251 and U87MG cells (data not shown), most likely because these rates are already very low. Western blot analysis indicated that pretreatment with Dex for 12 hours caused increased expressions of p-ERK1/2 and p-AKT in both U251 and U87MG cells at 24 hours (Figure 1B), with the most significant effect observed at 10 nM ($P < .01$ or $P < .001$).

3.2 | Effect of Dex on the migration and invasion of glioma cells and its underlying mechanisms

This study initially treated glioblastoma cells with Dex for 12 hours, then cells were cultured in a medium without Dex. We did not find any difference in the cell migration between the Dex-treated and the control groups even after 36 hours of culture (data not shown). Cell invasion was also unaffected by 10 nM Dex. ERK1/2 and AKT signalling pathways were involved in the cell invasion. This study initially treated glioblastoma cells with ERK1/2 and AKT inhibitors for 12 hours, then cells were cultured in medium without the inhibitors. The invasion of glioblastoma cells were notably inhibited at 24 hours after removing the inhibitors (Figure 2A, $P < .05$ or $P < .01$). Treatment
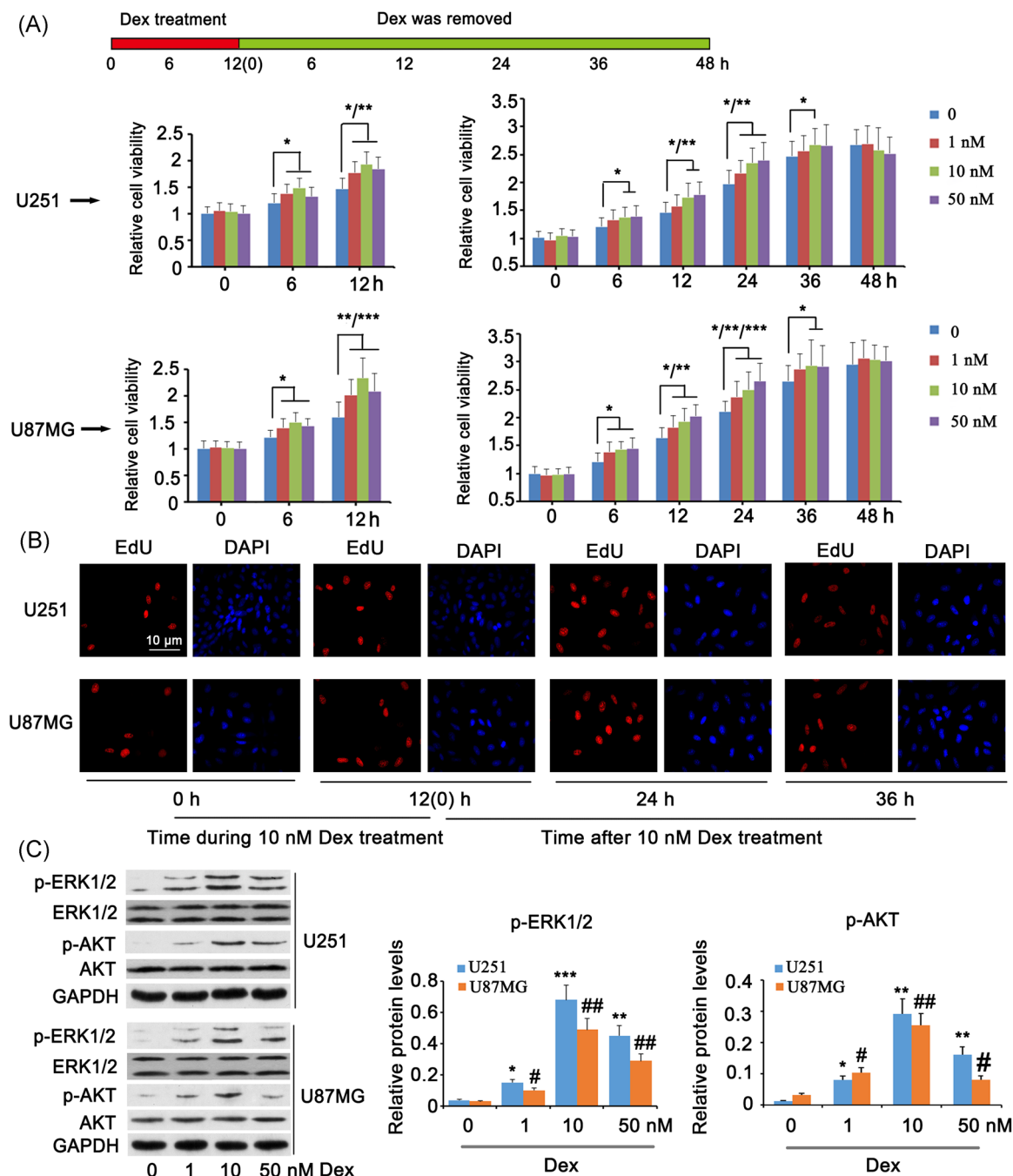
FIGURE 1 Effect of Dex on the growth of glioma cells. U251 and U87MG cells were treated with various doses of Dex (1, 10 and 50 nM) for 6 and 12 hours. The cells were then recultured in the Dex-free culture medium for 48 hours. Cell viability was assessed at different time points throughout. A, Cell viability assay. B, EdU staining assay. C, Western blot measurement. DAPI, 4′,6-diamidino-2-phenylindole; Dex, dexmedetomidine; EdU, 5-ethynyl-2′-deoxyuridine; ERK1/2, extracellular-signal-regulated kinase 1/2; GADPH, glyceraldehyde 3-phosphate dehydrogenase. *$P < .05$, **$P < .01$, ***$P < .001$, #$P < .05$, ##$P < .01$ vs control group

with 10 nM Dex in combination with ERK1/2 and AKT inhibitors also showed inhibited invasion of glioblastoma cells ($P < .05$). In addition, treatment with 50 nM Dex decreased the invasion of both U251 and U87MG cells. Intracellular protein expression of p-MLC was inhibited by treatment with 10 nM Dex and ERK1/2 inhibitor in combination (Figure 2B, $P < .05$), but not by 10 nM Dex alone. Treatment with Dex at a dose of 50 nM significantly decreased the amount of p-MLC in U251 and U87MG cells ($P < .05$). Intracellular Ca^{2+} concentration (Figure 2C) was also reduced following the treatment with 10 nM ($P < .05$) and 50 nM Dex ($P < .01$).
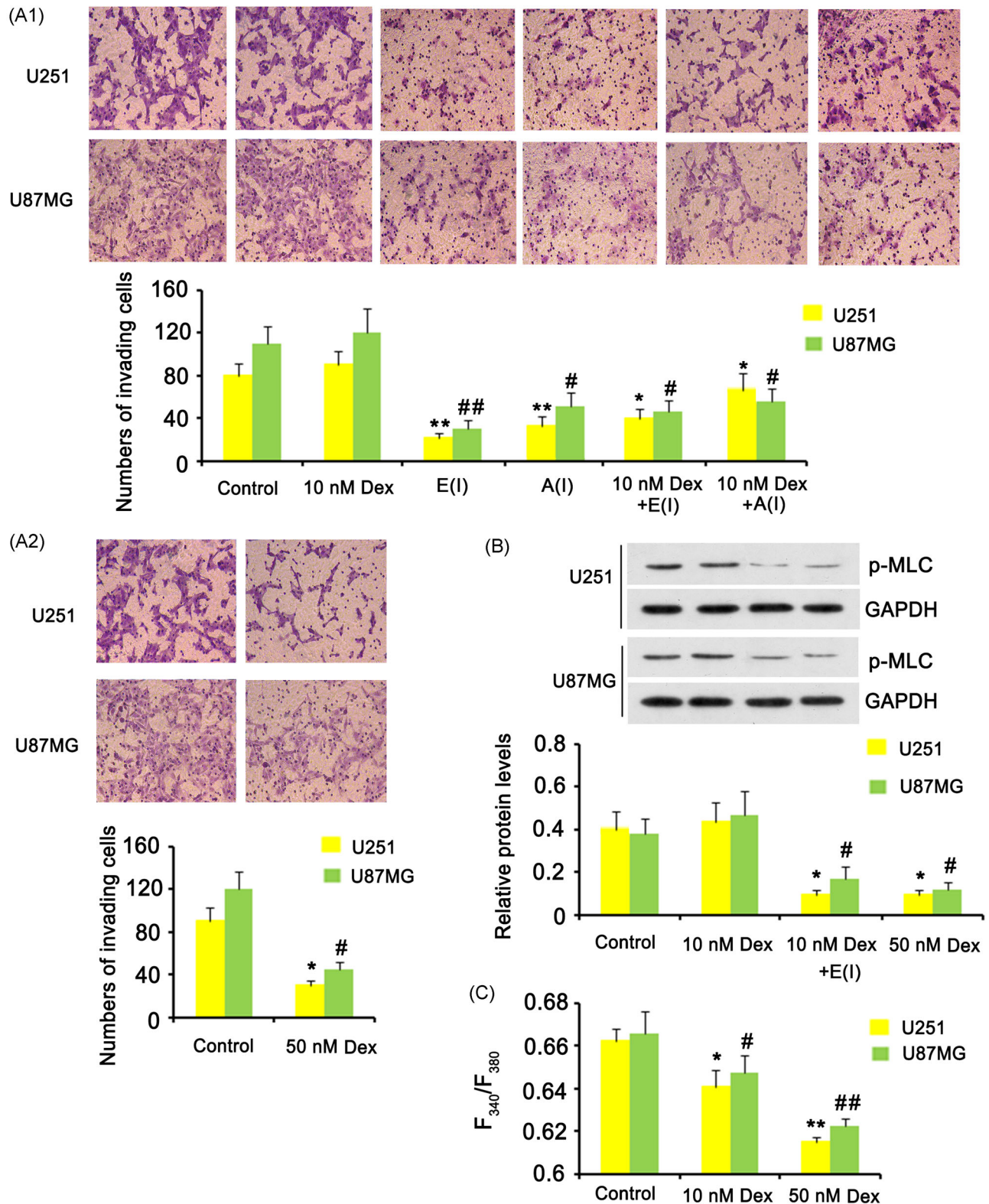
FIGURE 2 Effect of Dex on the migration and invasion of glioma cells. U251 and U87MG cells were treated with 10 nM Dex, 10 nM ERK1/2 inhibitor, 5 µM AKT inhibitor, 10 nM Dex + 10 nM ERK1/2 inhibitor, 10 nM Dex + 5 µM AKT inhibitor (A1) and 50 nM Dex (A2) for 12 hours, then the cells were cultured in a free medium without Dex and the inhibitors for 24 hours. A, Invasion assay. B, Western blot measurement. C, Measurement of intracellular Ca^{2+} concentration. A(I), AKT inhibitor; Dex, dexmedetomidine; E(I), ERK1/2 inhibitor; GADPH, glyceraldehyde 3-phosphate dehydrogenase; MLC, myosin light chain. $*P < .05$, $**P < .01$, $^{\#}P < .05$ vs control group

3.3 | Effect of Dex on the growth of DDP-treated glioma cells and its underlying mechanisms

The viabilities of U251 and U87MG cells were significantly impaired by DDP (Figure 3A, $P < .01$), however, pretreatment with 10 nM Dex or simultaneous treatment with 10 nM Dex and DDP attenuated this cell damage ($P < .05$). Conversely, pretreatment with 50 nM Dex increased the toxicity of DDP ($P < .05$). Furthermore, no significantly protective effect was observed during simultaneous treatment with 50 nM Dex and DDP. DDP caused a notable increase in the apoptotic rate of both cell lines (Figure 3B, $P < .01$), but this effect was attenuated by 10 nM Dex following both pretreatment and simultaneous administration ($P < .05$). Pretreatment with 50 nM Dex instead further elevated the DDP-induced increase in apoptotic rate, but this enhancement was not observed during simultaneous treatment with 50 nM Dex. Treatment with DDP notably elevated intracellular ROS (Figure 3C, $P < .01$) and p-p56 (Figure 3D, $P < .05$ or $P < .01$) levels. These increases were prevented by administration of Dex (10 and 50 nM) both before and during DDP treatment ($P < .05$ or $P < .01$).
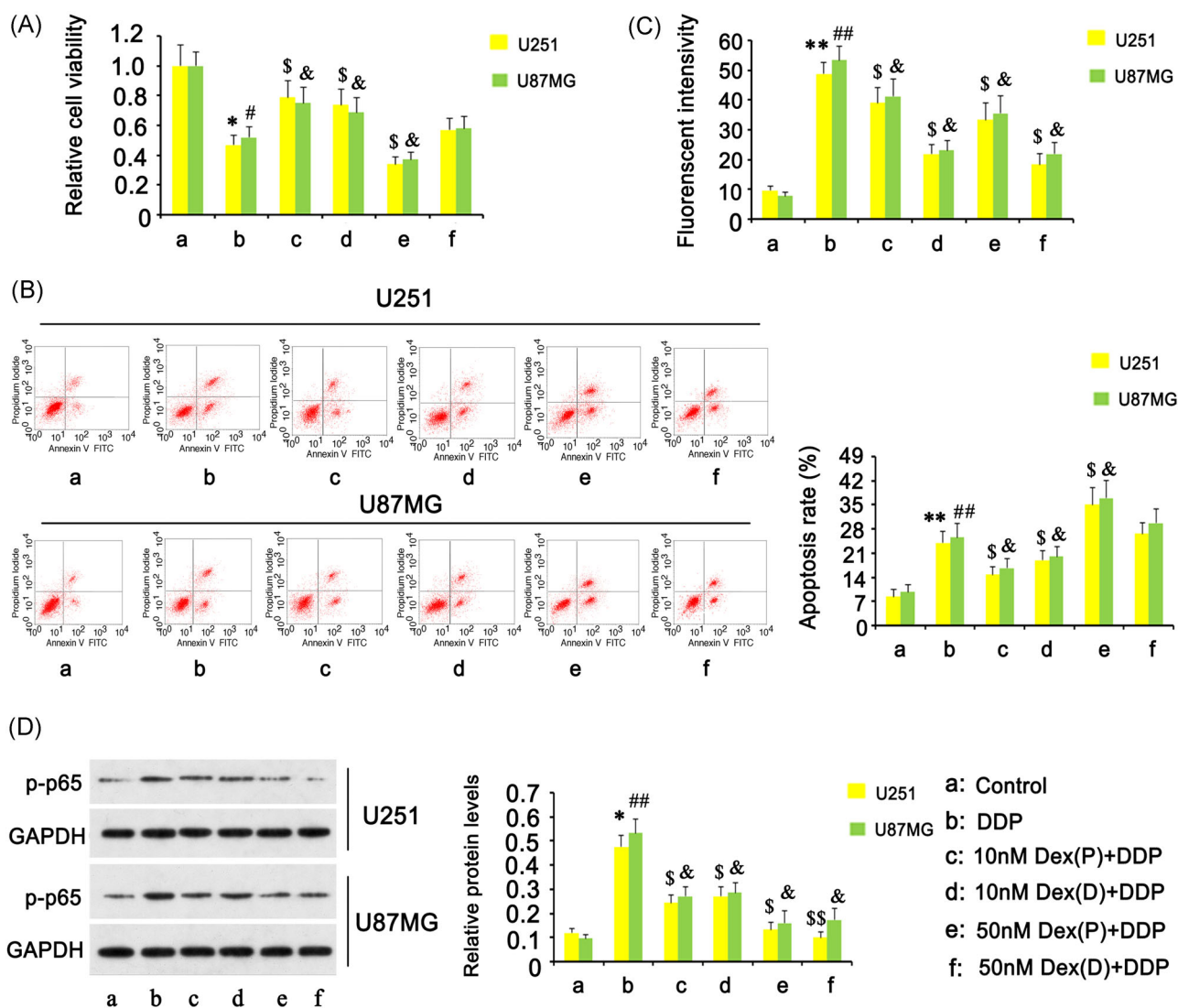

FIGURE 3 Effect of Dex on the growth of DDP-treated glioma cells. Dex was added to U251 and U87MG cells 12 hours before (processing mode one, P1) or simultaneously with (processing mode two, P2) treatment with 30 μM DDP for 12 hours to determine the protective effect of Dex. A series of assays were performed immediately after P1 and 12 hours after P2. A, Cell viability assay. B, Apoptosis assay. C, Measurement of intracellular ROS. D, Western blot measurement. DDP, cisplatin; Dex, dexmedetomidine; Dex(D), Dex was added during DDP treatment; Dex(P), Dex was added before DDP treatment; GADPH, glyceraldehyde 3-phosphate dehydrogenase; ROS, reactive oxygen species. *$P < .05$, **$P < .01$, #$P < .05$, ##$P < .01$ vs control group. $\$P < .05$, $\$\$P < .01$, $\&P < .05$ vs DDP treatment group

3.4 | Effect of Dex on the migration and invasion of DDP-treated glioma cells

DDP significantly inhibited the migration and invasion of U251 and U87MG cells ($P < .05$ or $P < .01$, Figure 4A and 4B). However, adding 10 nM Dex before or during DDP treatment partly restored these effect ($P < .05$) with the better effect observed in Dex added during DDP treatment. Treatment with Dex at 50 nM, before and during DDP insult, decreased the migration of U87MG cells ($P < .05$) and the invasion of both U251 and U87MG cells ($P < .05$).

3.5 | Effect of Dex on glioma tumour in nude mice that received DDP or not

The in vivo study showed that Dex did not significantly increase the glioma volume of U251 and U87MG cells (Figure 5A). The growth of glioma was inhibited by DDP ($P < .05$), which was not significantly affected by Dex either. As indicated by immunohistochemistry assay, ki67 staining of U251 and U87MG cells was not increased with the use of Dex, but it reduced as mice received DDP treatment ($P < .05$; Figure 5B). Treatment with Dex inhibited the reduction of ki67 staining caused by DDP
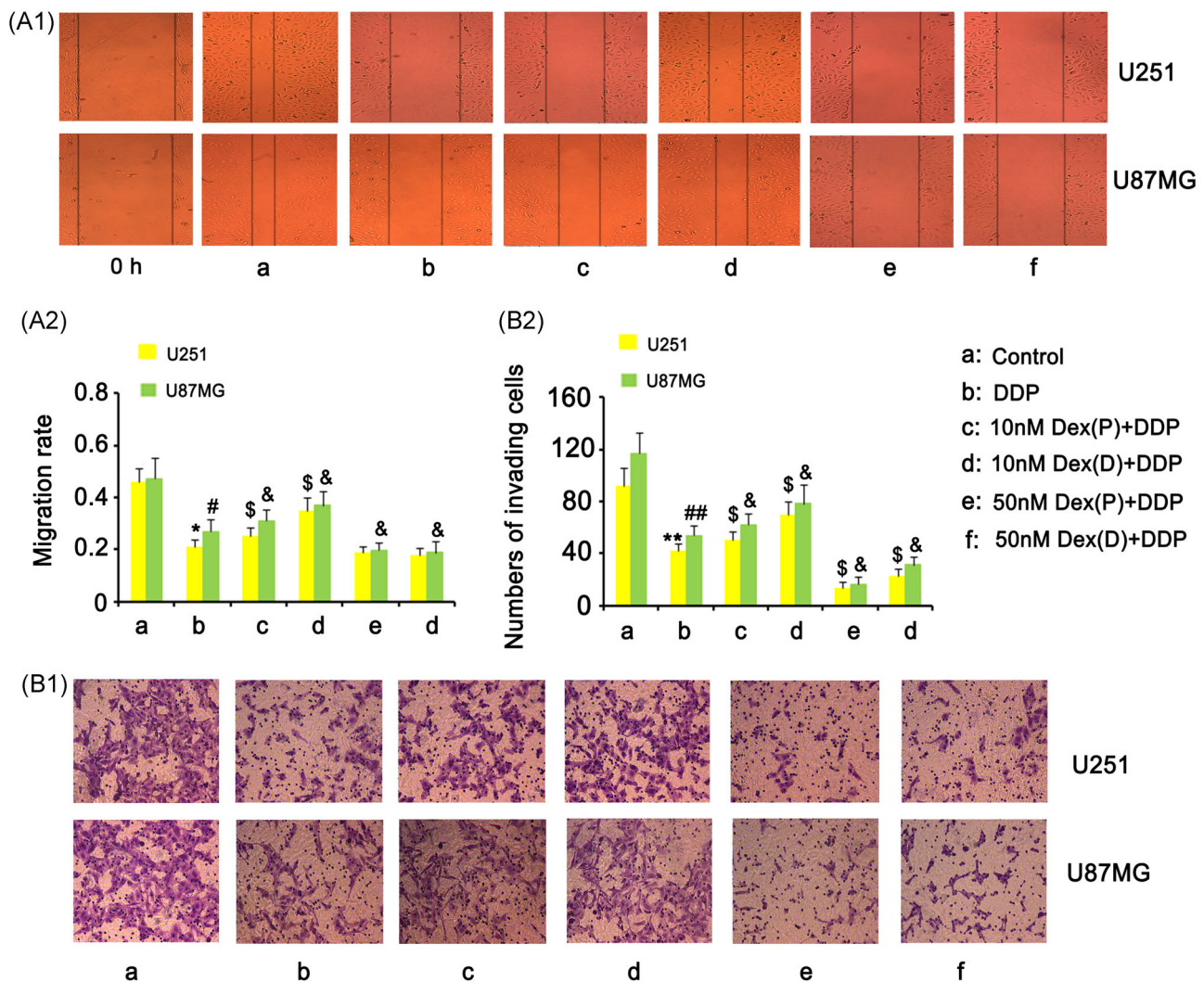

FIGURE 4 Effect of Dex on the migration and invasion of DDP-treated glioma cells. Dex was added to U251 and U87MG cells 12 hours before (processing mode one, P1) or simultaneously with (processing mode two, P2) treatment with DDP (#P4394; Sigma-Aldrich; Shanghai, China) for 12 hours to determine the protective effect of Dex. A series of assays were performed immediately after P1 and 12 hours after P2. A, Migration assay: panel A1 and A2 showed the pictures and bar chart, respectively. B, Invasion assay: panel B1 and B2 showed the pictures and bar chart, respectively. DDP, cisplatin; Dex, dexmedetomidine; Dex (D), Dex was added during DDP treatment; Dex (P), Dex was added before DDP treatment. *$P < .05$, **$P < .01$, #$P < .05$, ##$P < .01$ vs control group. $P < .05$, $$P < .01$, &$P < .05$ vs DDP treatment group
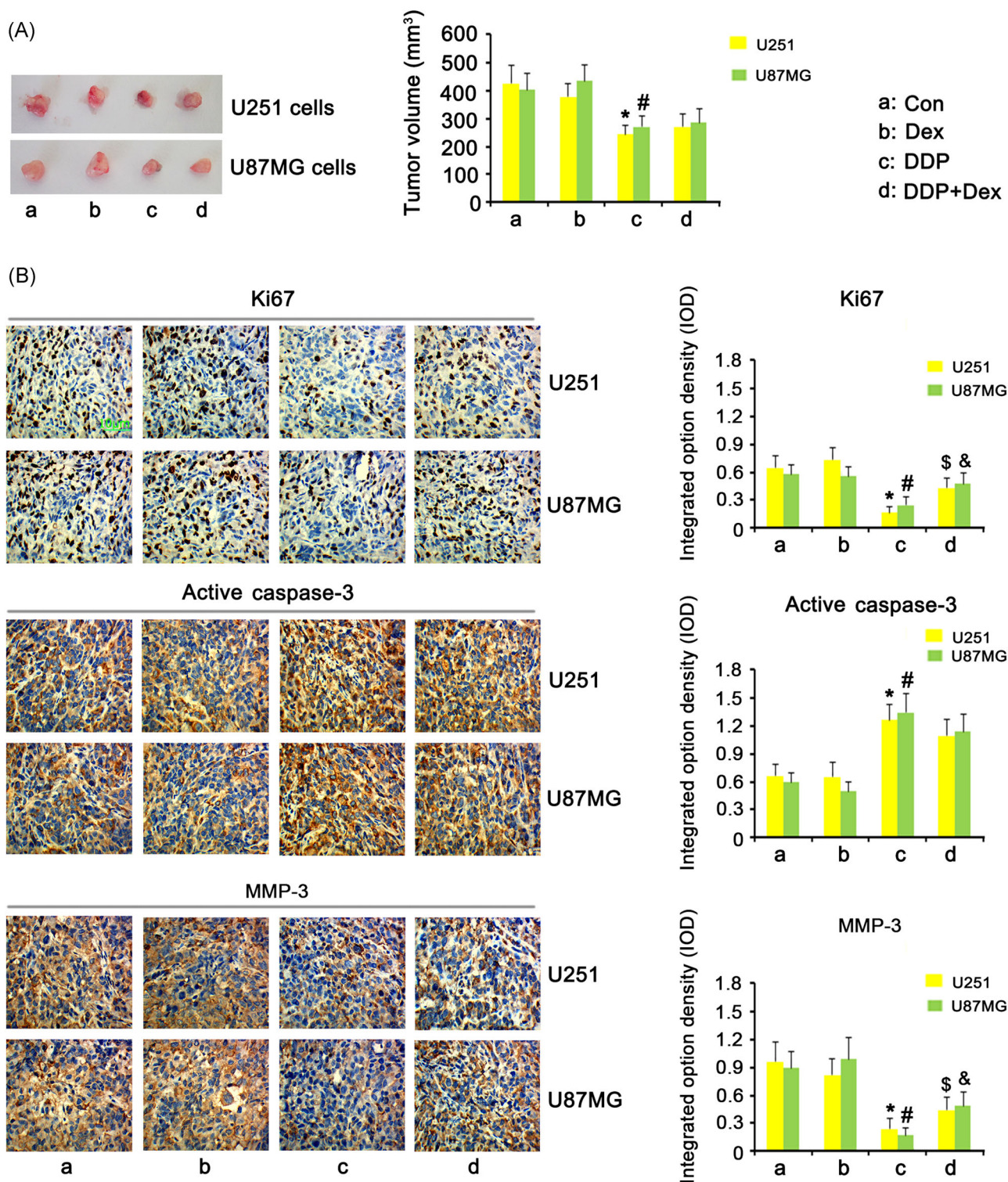
FIGURE 5 Effect of Dex on glioma tumour in nude mice that received DDP or not. Nude mice received a subcutaneous injection of U251 or U87MG cells (1×10^6). The mice 5 days after the implantation of U251 or U87MG cells received normal saline (as control), Dex (0.5 mg/kg, 0.1 mL/10 g; subcutaneous injection), DDP (4 mg/kg, 0.1 mL/10 g, intraperitoneal injection) or Dex + DDP per 5 days. A, Tumour volume evaluation. B, Immunohistochemistry assay. DDP, cisplatin; Dex, dexmedetomidine; MMP-3, matrix metalloproteinase-3. *$P < .05$ and #$P < .05$ vs control group; $$P < .05$ and &$P < .05$ vs DDP treatment group

($P < .05$ vs DDP group). Dex did not have notable effect on the abundance of active caspase-3 in glioma regardless of the treatment of mice with DDP or not, although treatment with DDP notably increased the abundance of active caspase-3 ($P < .05$). However, Dex blocked the DDP-mediated suppression of MMP-3 expression in the glioma ($P < .05$ vs DDP group).

4 | DISCUSSION

In clinical practice, it is possible that a few of glioma cells are residual even after the tumour resection surgery. Moreover, for patients in advanced glioma stage, glioma is unable to be completely removed by surgery, but it is commonly required the surgery to attenuate glioma-induced adverse symptoms such as intracranial haemorrhage and the increase of intracranial pressure. In these cases, Dex used during and after the surgery likely makes some influence on the growth and invasion of glioma.

Our in vitro study revealed that Dex at 10 nM promotes the growth and proliferation of human glioma U251 and U87MG cells, and that this promoting effect extends for a relatively short time after its removal. Earlier research has shown that treatment with Dex is associated with an increase in [3H]thymidine incorporation into breast cancer cells and inhibition of cell death, suggesting that Dex stimulates proliferation.[16] Castillo et al[17] recently found that a mitogenic autocrine/paracrine prolactin loop mediates the stimulation of breast cancer cell proliferation by Dex. The growth-promoting effect of Dex has also recently been reported in human glioma (H4) and lung carcinoma (A549) cells.[18] According to the report, H4 cell proliferation was increased two-fold with the administration of 1 nM Dex.[18] Our results also showed an increase in viability of glioma U251 and U87MG cells triggered by higher concentrations (10 and 50 nM) of Dex. In addition, although Dex was removed after 12 hours of treatment, the U251 and U87MG cells continued to display faster proliferation than vehicle control cells for at least 24 hours. Cell proliferation induced by Dex may be related to the observed activation of PI3K, Akt and ERK1/2, the signalling molecules downstream of α_2-ARs.[14,19] The present study showed an increase in phosphorylation levels of Akt, and ERK1/2 in glioma cells after exposure to Dex. The effects of Dex on the proliferation of various tumour hence deserve attention.

Dex has been shown to potentiate the migration of glioma H4 cells,[18] but this effect was rather weak in the U251 and U87MG cells in our experiments. In the wound healing assay, Dex only moderately increased the migration of U251 and U87MG cells. High concentrations (50 nM) of Dex even decreased the invasion of U251 and U87MG cells in the invasion assay. Similarly, a study showed that Dex induces cell-cycle progression and cell proliferation of PC12 cells (a type of neuronal pheochromocytoma rat cell) but suppresses their cell migration and invasion abilities.[20] The underlying molecular basis is likely due to the reduction of COL3A1 levels by the upregulation of miR-let-7b.[20] Wangc et al[21] reported that Dex inhibits both the proliferation and migration of osteosarcoma cells by upregulating the expression of miR-520a-3p. The upregulated miR-520a-3p suppressed the expression of AKT, p-AKT, p-mTOR and p-ERK1/2. These data are inconsistent with the findings of the present study, so it is likely that Dex confers its effects by very different molecular mechanisms in glioma and osteosarcoma cells.

It has been established that ERK1/2 and AKT signalling pathways play key roles in promoting cell migration and invasion. ERK1/2 functions as an important mediator for a variety of invasion-related processes, including cytoskeleton rearrangement, myosin-mediated cell contractility, tail retraction and focal adhesions by activating RhoA GTPase/ROCK signalling.[22] However, the phosphorylation level of MLC, which is direct downstream of RhoA GTPase/ROCK signalling, were not notably changed in U251 and U87MG cells following Dex treatment. It is possible that Dex affects a different signalling pathway that interferes with or counteracts the ERK1/2-promotion of RhoA GTPase/ROCK cascades. This possibility is supported by our finding that Dex treatment decreased intracellular Ca^{2+} concentration. The concentration of Ca^{2+} in the cytoplasm has been positively correlated with the migration and invasion of various cancer cells because Ca^{2+} can function as an important intracellular messenger regulating cell invasion dependent on RhoA GTPase/ROCK or not.[23,24] There is another possibility that the RhoA GTPase/ROCK signal may already be overactivated in these cells, a phenomenon commonly observed in advanced cancer compared with early stage cancer, and activation of ERK1/2 fails to further stimulate this signal. In the present study, when ERK1/2 or AKT inhibitor was used, cell invasion was suppressed regardless of Dex treatment or not.

The present study further demonstrated that a low dose (10 nM) of Dex protects U251 and U87MG cells from DDP toxicity, whether the dose is administered before or with DDP. However, a high concentration (50 nM) of Dex conversely promoted DDP-induced toxicity. In most previous studies, Dex was found to confer protection against anti-cancer drugs, hypoxia and ischaemic/reperfusion injury in multiple cell lines.[9,10,15] This protection was conferred through multiple signalling molecules and

pathways, including NF-κB, ERK1/2, Nrf2, JAK2/STAT3 and p38/NO, all of which are directly or indirectly regulated by α_2-AR. Previous studies have reported that α_2-AR-mediated inhibition of NF-κB is responsible for Dex protection against DDP toxicity in kidneys.[15] Inhibition of NF-κB decreases the expression of tumour necrosis factor-α, interleukin-1β (IL-1β), IL-6 and monocyte chemoattractant protein-1 and suppresses the infiltration of macrophages and T cells into the kidneys, thus limiting local inflammation. By analysing the expression of p-p65, our experiments showed that DDP-induced activation of NF-κB was also disrupted by Dex in U251 and U87MG cells. However, NF-κB has been confirmed to play an important role in the chemoresistance of cancer cells by various mechanisms, including activation of ABC transporters and upregulation of the survivin protein.[25,26] Therefore, the inhibition of NF-κB would be expected to increase glioma cell susceptibility to DDP, which may explain why high concentrations of Dex promoted DDP toxicity. The protection conferred by Dex at a low dose is likely associated with the modulation of other signalling molecules and the elevation of antioxidative capacity. We found that Dex hindered the DDP-induced increase in intracellular ROS. The activation of Nrf2 has been previously reported to mediate the antioxidative action of Dex.[27]

The effects of Dex on the migration and invasion of DDP-treated U251 and U87MG cells varied heavily with dosage and time. DDP significantly inhibited the migration and invasion of both cell lines, but adding 10 nM Dex simultaneously with DDP partly restored these behaviours. In contrast, pretreatment with 10 nM Dex conferred no protective effect on migration and invasion. Administration of Dex at 50 nM, both before and during DDP treatment, potentiated the inhibitory effect of DDP on both migration and invasion. Due to the complicated effects conferred by Dex on the expression and activation of multiple signalling molecules, it is difficult to elucidate exactly how Dex exerts its different effects. However, our study provided some clues to the underlying mechanisms. Dex appeared to block DDP activation of NF-κB. Substantial evidence has shown that NF-κB promotes cell migration and invasion by increasing the expression of MMPs, among other mechanisms.[28,29] A particularly interesting result of our study is the finding that DDP suppressed cell migration and invasion despite promotion of NF-κB activity. It is likely that this is a result of DDP influencing other mechanistic routes that inhibit cell migration and invasion, and that this inhibitory action is stronger than the promoting effects of NF-κB. Thus, Dex inhibition of NF-κB activation by DDP may further negatively impact migration and invasion.

The in vivo study showed that Dex had no significant effect on the tumour growth regardless of the treatment of DDP or not. Besides, Dex failed to block DDP-induced activation of caspase-3, suggesting a moderate effect of Dex on inhibiting the apoptosis at least in vivo; but Dex blocked the inhibitory effect of DDP on the expression of Ki67 and MMP-3. As to why Dex did not significant promote the tumour growth, we hypothesised that Dex was degraded much faster in vivo than in vitro, or the dosage of Dex used in vivo is too low to enhance the growth of tumour. The present study using a relative low dosage of Dex in nude mice is due to the strong sedative effect of Dex. High dosage of Dex could lead to the sleepiness of mice and thus inactivity. Consequently, it is unclear whether the growth of tumour is influenced by the Dex directly or by the sedative effect of Dex. Further study is suggested to compare the effect of different anaesthetics at various dosages on the growth of tumour, which can eliminate the interference from their sedative effect.

In conclusion, this study provides evidence of the regulatory effects of Dex on proliferation, invasion and chemosensitivity of glioma cells, and outlines potential mechanisms for these effects. Although these hallmarks of glioma cells were notably affected by Dex in vitro, glioma growth was not significantly changed by Dex at least at a low dosage in vivo. The effect of Dex on glioma proliferation and invasion in a clinical setting still needs further study.

CONFLICT OF INTERESTS

The authors declare that there are no conflict of interests.

ORCID

Hao Wu http://orcid.org/0000-0002-9544-5488

REFERENCES

1. Ostrom QT, Gittleman H, Stetson L, Virk SM, Barnholtz-Sloan JS. Epidemiology of gliomas. *Cancer Treat Res.* 2015; 163:1-14.
2. Yang P, Wang Y, Peng X, et al. Management and survival rates in patients with glioma in China (2004-2010): a retrospective study from a single-institution. *J Neurooncol.* 2013;113(2):259-266.
3. Wangb L, Peng Y, Peng J, et al. Tramadol attenuates the sensitivity of glioblastoma to temozolomide through the suppression of Cx43-mediated gap junction intercellular communication. *Int J Oncol.* 2018;52(1):295-304.
4. Zhang Y, Wang X, Wang Q, Ge H, Tao L. Propofol depresses cisplatin cytotoxicity via the inhibition of gap junctions. *Mol Med Rep.* 2016;13(6):4715-4720.

5. Hurmath FK, Mittal M, Ramaswamy P, Umamaheswara Rao GS, Dalavaikodihalli Nanjaiah N. Sevoflurane and thiopental preconditioning attenuates the migration and activity of MMP-2 in U87MG glioma cells. *Neurochem Int.* 2016;94:32-38.

6. Wang X, Li Y, Wang H, et al. Propofol inhibits invasion and proliferation of C6 glioma cells by regulating the Ca^{2+} permeable AMPA receptor-system xc-pathway. *Toxicol In Vitro.* 2017;44:57-65.

7. Yi W, Li D, Guo Y, Zhang Y, Huang B, Li X. Sevoflurane inhibits the migration and invasion of glioma cells by upregulating microRNA-637. *Int J Mol Med.* 2016;38(6):1857-1863.

8. Leng T, Lin S, Xiong Z, Lin J. Lidocaine suppresses glioma cell proliferation by inhibiting TRPM7 channels. *Int J Physiol Pathophysiol Pharmacol.* 2017;9(2):8-15.

9. Cakir sancaktar N, Altinbas A, Cekic B. Protective role of dexmedetomidine on ileum and kidney damage caused by mesenchymal ischaemia in rats. *Turk J Anesth Reanim.* 2018;46(6):470-477.

10. Sun Y, Jiang C, Jiang J, Qiu L. Dexmedetomidine protects mice against myocardium ischaemic/reperfusion injury by activating an AMPK/PI3K/Akt/eNOS pathway. *Clin Exp Pharmacol Physiol.* 2017;44(9):946-953.

11. Xu H, Zhao B, She Y, Song X. Dexmedetomidine ameliorates lidocaine-induced spinal neurotoxicity via inhibiting glutamate release and the PKC pathway. *Neurotoxicology.* 2018;69:77-83.

12. Wang SL, Duan L, Xia B, Liu Z, Wang Y, Wang GM. Dexmedetomidine preconditioning plays a neuroprotective role and suppresses TLR4/NF-κB pathways model of cerebral ischemia reperfusion. *Biomed Pharmacother.* 2017;93:1337-1342.

13. Lavon H, Matzner P, Benbenishty A, et al. Dexmedetomidine promotes metastasis in rodent models of breast, lung, and colon cancers. *Br J Anaesth.* 2018;120(1):188-196.

14. Xia M, Ji NN, Duan ML, et al. Dexmedetomidine regulate the malignancy of breast cancer cells by activating α2-adrenoceptor/ERK signaling pathway. *Eur Rev Med Pharmacol Sci.* 2016;20(16):3500-3506.

15. Liang H, Liu HZ, Wang HB, Zhong JY, Yang CX, Zhang B. Dexmedetomidine protects against cisplatin-induced acute kidney injury in mice through regulating apoptosis and inflammation. *Inflamm Res.* 2017;66(5):399-411.

16. Bruzzone A, Piñero CP, Castillo LF, et al. α2-Adrenoceptor action on cell proliferation and mammary tumour growth in mice: α2-Adrenoceptor action on mammary tumours. *Br J Pharmacol.* 2008;155(4):494-504.

17. Castillo LF, Rivero EM, Goffin V, Lüthy IA. Alpha2-adrenoceptor agonists trigger prolactin signaling in breast cancer cells. *Cell Signal.* 2017;34:76-85.

18. Wang C, Datoo T, Zhao H, et al. Midazolam and dexmedetomidine affect neuroglioma and lung carcinoma cell biology in vitro and in vivo. *Anesthesiology.* 2018;129(5):1000-1014.

19. Cheng X, Hu J, Wang Y, et al. Effects of dexmedetomidine postconditioning on myocardial ischemia/reperfusion injury in diabetic rats: role of the PI3K/Akt-dependent signaling pathway. *J Diabetes Res.* 2018;2018:1-10.

20. Wang Q, She Y, Bi X, Zhao B, Ruan X, Tan Y. Dexmedetomidine protects pc12 cells from lidocaine-induced cytotoxicity through downregulation of COL3A1 mediated by miR-let-7b. *DNA Cell Biol.* 2017;36(7):518-528.

21. Wang X, Xu Y, Chen X, Xiao J. Dexmedetomidine inhibits osteosarcoma cell proliferation and migration, and promotes apoptosis by regulating miR-520a-3p. *Oncol Res.* 2018;26(3):495-502.

22. Narumiya S, Tanji M, Ishizaki T. Rho signaling, ROCK and mDia1, in transformation, metastasis and invasion. *Cancer Metastasis Rev.* 2009;28(1-2):65-76.

23. Stadler S, Nguyen CH, Schachner H, et al. Colon cancer cell-derived 12(S)-HETE induces the retraction of cancer-associated fibroblast via MLC2, RHO/ROCK and Ca^{2+} signalling. *Cell Mol Life Sci.* 2017;74(10):1907-1921.

24. Velaei K, Samadi N, Soltani S, Barazvan B, Soleimani Rad J. NFκBP65 transcription factor modulates resistance to doxorubicin through ABC transporters in breast cancer. *Breast Cancer.* 2017;24(4):552-561.

25. Zheng HC. The molecular mechanisms of chemoresistance in cancers. *Oncotarget.* 2017;8(35):59950-59964.

26. Kugelmann D, Rotkopf LT, Radeva MY, Garcia-Ponce A, Walter E, Waschke J. Histamine causes endothelial barrier disruption via Ca^{2+}-mediated RhoA activation and tension at adherens junctions. *Sci Rep.* 2018;8(1):13229.

27. Chen Z, Ding T, Ma CG. Dexmedetomidine (DEX) protects against hepatic ischemia/reperfusion (I/R) injury by suppressing inflammation and oxidative stress in NLRC5 deficient mice. *Biochem Biophys Res Commun.* 2017;493(2):1143-1150.

28. Song ZB, Ni JS, Wu P, et al. Testes-specific protease 50 promotes cell invasion and metastasis by increasing NF-kappaB-dependent matrix metalloproteinase-9 expression. *Cell Death Dis.* 2015;6:e1703.

29. Cai J, Li R, Xu X, et al. URGCP promotes non-small cell lung cancer invasiveness by activating the NF-κB-MMP-9 pathway. *Oncotarget.* 2015;6(34):36489-36504.